

---

# Policy Gradient Bayesian Robust Optimization for Imitation Learning

---

Zaynah Javed<sup>\*1</sup> Daniel S. Brown<sup>\*1</sup> Satvik Sharma<sup>1</sup> Jerry Zhu<sup>1</sup> Ashwin Balakrishna<sup>1</sup> Marek Petrik<sup>2</sup>  
Anca D. Dragan<sup>1</sup> Ken Goldberg<sup>1</sup>

## Abstract

The difficulty in specifying rewards for many real-world problems has led to an increased focus on learning rewards from human feedback, such as demonstrations. However, there are often many different reward functions that explain the human feedback, leaving agents with *uncertainty* over what the true reward function is. While most policy optimization approaches handle this uncertainty by optimizing for expected performance, many applications demand risk-averse behavior. We derive a novel policy gradient-style robust optimization approach, PG-BROIL, that optimizes a soft-robust objective that balances expected performance and risk. To the best of our knowledge, PG-BROIL is the first policy optimization algorithm robust to a distribution of reward hypotheses which can scale to continuous MDPs. Results suggest that PG-BROIL can produce a family of behaviors ranging from risk-neutral to risk-averse and outperforms state-of-the-art imitation learning algorithms when learning from ambiguous demonstrations by hedging against uncertainty, rather than seeking to uniquely identify the demonstrator’s reward function.

## 1. Introduction

We consider the following question: *How should an intelligent agent act if it has epistemic uncertainty over its objective function?* In the fields of reinforcement learning (RL) and optimal control, researchers and practitioners typically assume a known reward or cost function, which is then optimized to obtain a policy. However, even in settings where the reward function is specified, it is usually only a best approximation of the objective function that a human thinks will lead to desirable behavior. Furthermore,

human-designed reward functions are also often augmented with human feedback. This may also result in reward uncertainty since human feedback, be it in the form of policy shaping (Griffith et al., 2013), reward shaping (Knox & Stone, 2012), or a hand-designed reward function (Hadfield-Menell et al., 2017; Ratner et al., 2018), can fail to perfectly disambiguate the human’s intent true (Amodei et al., 2016).

Reward function ambiguity is also a key problem in imitation learning (Hussein et al., 2017; Osa et al., 2018), in which an agent seeks to learn a policy from demonstrations without access to the reward function that motivated the demonstrations. While many imitation learning approaches either sidestep learning a reward function and directly seek to imitate demonstrations (Pomerleau, 1991; Torabi et al., 2018) or take a maximum likelihood (Choi & Kim, 2011; Brown et al., 2019) or maximum entropy approach to learning a reward function (Ziebart et al., 2008; Fu et al., 2017), we believe that an imitation learning agent should explicitly reason about uncertainty over the true reward function to avoid misalignment with the demonstrator’s objectives (Hadfield-Menell et al., 2017; Brown et al., 2020a). Bayesian inverse reinforcement learning (IRL) methods (Ramachandran & Amir, 2007) seek a posterior distribution over likely reward functions given demonstrations, but often perform policy optimization using the expected reward function or MAP reward function (Ramachandran & Amir, 2007; Choi & Kim, 2011; Ratner et al., 2018; Brown et al., 2020a). However, in many real world settings such as robotics, finance, and healthcare, we desire a policy which is robust to uncertainty over the true reward function.

Prior work on risk-averse and robust policy optimization in reinforcement learning has mainly focused on robustness to uncertainty over the true dynamics of the environment, but assumes a known reward function (Garcia & Fernández, 2015; Tamar et al., 2015; Tang et al., 2020; Derman et al., 2018; Lobo et al., 2020; Thananjeyan et al., 2021). Some work addresses robust policy optimization under reward function uncertainty by taking a maxmin approach and optimizing a policy that is robust under the worst-case reward function (Syed et al., 2008; Regan & Boutilier, 2009; Hadfield-Menell et al., 2017; Huang et al., 2018). However, these approaches are limited to tabular domains, and maxmin approaches have been shown to sometimes lead to

---

<sup>1</sup>EECS Department, University of California, Berkeley <sup>2</sup>CS Department, University of New Hampshire. Correspondence to: Daniel Brown <dsbrown@berkeley.edu>.

incorrect and overly pessimistic policy evaluations (Brown & Niekum, 2018). As an alternative to maxmin approaches, recent work (Brown et al., 2020b) proposed a linear programming approach, BROIL: Bayesian Robust Optimization for Imitation Learning, that balances risk-aversion (in terms of Conditional Value at Risk (Rockafellar et al., 2000)) and expected performance. This approach supports a family of solutions depending on the risk-sensitivity of the application domain. However, as their approach is built on linear programming, it cannot be applied in MDPs with continuous state and action spaces and unknown dynamics.

In this work, we introduce a novel policy optimization approach that enables varying degrees of risk-sensitivity by reasoning about reward uncertainty while scaling to continuous MDPs with unknown dynamics. As in Brown et al. (2020b), we present an approach which reasons simultaneously about risk-aversion (in terms of Conditional Value at Risk (Rockafellar et al., 2000)) and expected performance and balances the two. However, to enable such reasoning in continuous spaces, we make a key observation: the Conditional Value at Risk objective supports efficient computation of an approximate subgradient, which can then be used in a policy gradient method. This makes it possible to use any policy gradient algorithm, such as TRPO (Schulman et al., 2017a) or PPO (Schulman et al., 2017b) to learn policies which are robust to reward uncertainty, resulting in an efficient and scalable algorithm. To the best of our knowledge, our proposed algorithm, Policy Gradient Bayesian Robust Optimization for Imitation Learning (PG-BROIL), is the first policy optimization algorithm robust to a distribution of reward hypotheses that can scale to complex MDPs with continuous state and action spaces.

To evaluate PG-BROIL, we consider settings where there is uncertainty over the true reward function. We first examine the setting where we have an a priori distribution over reward functions and find that PG-BROIL is able to optimize policies that effectively trade-off between expected and worst-case performance. Then, we leverage recent advances in efficient Bayesian reward inference (Brown et al., 2020a) to infer a posterior over reward functions from preferences over demonstrated trajectories. While other approaches which do not reason about reward uncertainty overfit to a single reward function hypothesis, PG-BROIL optimizes a policy that hedges against multiple reward function hypotheses. When there is high reward function ambiguity due to limited demonstrations, we find that PG-BROIL results in significant performance improvements over other state-of-the-art imitation learning methods.

## 2. Related Work

**Reinforcement Learning:** There has been significant recent interest in safe and robust reinforcement learn-

ing (Garcia & Fernández, 2015); however, most approaches are only robust with respect to noise in transition dynamics and only consider optimizing a policy with respect to a single reward function. Existing approaches reason about risk measures with respect to a single task rewards (Heger, 1994; Shen et al., 2014; Tamar et al., 2014; Tang et al., 2019), establish convergence to safe regions of the MDP (Thananjeyan et al., 2020b;a), or optimize a policy to avoid constraint violations (Achiam et al., 2017; Fisac et al., 2018; Thananjeyan et al., 2021).

In this paper, we develop a reinforcement learning algorithm which reasons about risk with respect to a belief distribution over the task reward function. We focus on being robust to tail risk by optimizing for conditional value at risk (Rockafellar et al., 2000). However, unlike prior work (Heger, 1994; Shen et al., 2014; Tamar et al., 2014; 2015; Tang et al., 2019; Zhang et al., 2021), which focuses on risk with respect to a known reward function and stochastic transitions, we consider policy optimization when there is epistemic uncertainty over the reward function itself. We formulate a soft-robustness approach that blends optimizing for expected performance and optimizing for the conditional value at risk. Recent work also considers soft-robust objectives when there is uncertainty over the correct transition model of the MDP (Lobo et al., 2020; Russel et al., 2020), rather than uncertainty over the true reward function.

**Imitation Learning:** Imitation learning approaches vary widely in reasoning about reward uncertainty. Behavioral cloning approaches simply learn to imitate the actions of the demonstrator, resulting in quadratic regret (Ross & Bagnell, 2010). DAgger (Ross et al., 2011) achieves sublinear regret by repeatedly soliciting human action labels in an online fashion. While there has been work on safe variants of DAgger (Zhang & Cho, 2016; Hoque et al., 2021), these methods only enable robust policy learning by asymptotically converging to the policy of the demonstrator, and always assume access to an expert human supervisor.

Inverse reinforcement learning (IRL) methods are another way of performing imitation learning (Arora & Doshi, 2018), where the learning agent seeks to achieve better sample efficiency and generalization by learning a reward function which is then optimized to obtain a policy. However, most inverse reinforcement learning methods only result in a point-estimate of the demonstrator’s reward function (Abbeel & Ng, 2004; Ziebart et al., 2008; Fu et al., 2017; Brown et al., 2019). Risk-sensitive IRL methods (Lacotte et al., 2018; Majumdar et al., 2017; Santara et al., 2018) assume risk-averse experts and focus on optimizing policies that match the risk-aversion of the demonstrator; however, these methods focus on the aleatoric risk induced by transition probabilities and there is no clear way to adapt risk-averse IRL to the Bayesian robust setting, where the objective is to be robust

to epistemic risk over reward hypotheses rather than risk with respect to stochasticity in the dynamics. Bayesian IRL approaches explicitly learn a distribution over reward functions conditioned on the demonstrations, but usually only optimize a policy for the expected reward function or MAP reward function under this distribution (Ramachandran & Amir, 2007; Choi & Kim, 2011; Brown et al., 2020a).

We seek to optimize a policy that is robust to epistemic uncertainty in the true reward function of an MDP. Prior work on robust imitation learning has primarily focused on maxmin approaches which seek to optimize a policy for an adversarial worst-case reward function (Syed et al., 2008; Ho & Ermon, 2016; Regan & Boutilier, 2009; Hadfield-Menell et al., 2017; Huang et al., 2018). However, these approaches can learn overly pessimistic behaviors (Brown & Niekum, 2018) and existing approaches assume discrete MDPs with known transition dynamics (Syed et al., 2008; Regan & Boutilier, 2009; Hadfield-Menell et al., 2017) or require fully solving an MDP hundreds of times (Huang et al., 2018), effectively limiting these approaches to discrete domains. Recently, (Brown et al., 2020b) proposed a method for robust Bayesian optimization for imitation learning (BROIL), which optimizes a soft-robust objective that balances expected performance with conditional value at risk (Rockafellar et al., 2000). However, their approach is limited to discrete state and action spaces and known transition dynamics. By contrast, we derive a novel policy gradient approach which enables robust policy optimization with respect to reward function uncertainty for domains with continuous states and action and unknown dynamics.

### 3. Preliminaries and Notation

#### 3.1. Markov Decision Processes

We model the environment as a Markov Decision Process (MDP) (Puterman, 2005). An MDP is a tuple  $(\mathcal{S}, \mathcal{A}, r, P, \gamma, p_0)$ , with state space  $\mathcal{S}$ , action space  $\mathcal{A}$ , reward function  $r : \mathcal{S} \times \mathcal{A} \rightarrow \mathbb{R}$ , transition dynamics  $P : \mathcal{S} \times \mathcal{A} \times \mathcal{S} \rightarrow [0, 1]$ , discount factor  $\gamma \in [0, 1)$ , and initial state distribution  $p_0$ . We consider stochastic policies  $\pi : \mathcal{S} \times \mathcal{A} \rightarrow [0, 1]$  which output a distribution over  $\mathcal{A}$  conditioned on a state  $s \in \mathcal{S}$ . We denote the expected return of a policy  $\pi$  under reward function  $r$  as  $v(\pi, r) = \mathbb{E}_{\tau \sim \pi_\theta} [r(\tau)]$ .

#### 3.2. Distributions over Reward Functions

We are interested in solving MDPs when there is epistemic uncertainty over the true reward function. When we refer to the reward function as a random variable we will use  $R$ , and will use  $r$  to denote a specific model of the reward function. Reward functions are often parameterized as a linear combination of known features (Abbeel & Ng, 2004; Ziebart et al., 2008; Sadigh et al., 2017) or as a deep neural network

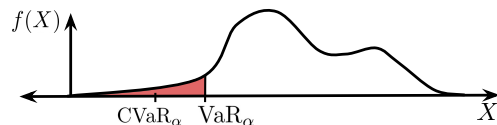


Figure 1. The pdf  $f(X)$  of a random variable  $X$ .  $\text{VaR}_\alpha$  measures the  $(1 - \alpha)$ -quantile outcome.  $\text{CVaR}_\alpha$  measures the expectation given that we only consider values less than the  $\text{VaR}_\alpha$ .

(Ho & Ermon, 2016; Fu et al., 2017). Thus, we can model uncertainty in the reward function as a distribution over  $R$ , or, equivalently, as a distribution over the reward function parameters. This distribution could be a prior distribution  $\mathbb{P}(R)$  that the agent learns from previous tasks (Xu et al., 2019). Alternatively, the distribution could be the posterior distribution  $\mathbb{P}(R | D)$  learned via Bayesian inverse reinforcement learning (Ramachandran & Amir, 2007) given demonstrations  $D$ , the posterior distribution  $\mathbb{P}(R | \mathcal{P}, D)$  given preferences  $\mathcal{P}$  over demonstrations (Sadigh et al., 2017; Brown et al., 2020a), or the posterior distribution  $\mathbb{P}(R | r')$  learned via inverse reward design given a human-specified proxy reward  $r'$  (Hadfield-Menell et al., 2017; Ratner et al., 2018). This distribution is typically only available via sampling techniques such as Markov chain Monte Carlo (MCMC) sampling (Ramachandran & Amir, 2007; Hadfield-Menell et al., 2017; Brown et al., 2020a).

#### 3.3. Risk Measures

We are interested in robust policy optimization with respect to a distribution over the performance of the policy induced by a distribution over possible reward functions. Consider a policy  $\pi$  and a reward distribution  $\mathbb{P}(R)$ . Together,  $\pi$  and  $\mathbb{P}(R)$  induce a distribution over the expected return of the policy,  $v(\pi, R), R \sim \mathbb{P}(R)$ . We seek a robust policy that minimizes tail risk, given some risk measure, under the induced distribution  $v$ . Figure 1 visualizes two common risk measures: value at risk (VaR) and conditional value at risk (CVaR), for a general random variable  $X$ . In our setting,  $X$  corresponds to the expected return,  $v(\pi, R)$ , of a policy  $\pi$  under the reward function random variable  $R$ , and the objective is to minimize the tail risk (visualized in red).

##### 3.3.1. VALUE AT RISK

Given a risk-aversion parameter  $\alpha \in [0, 1]$ , the  $\text{VaR}_\alpha$  of a random variable  $X$  is the  $(1 - \alpha)$ -quantile outcome:

$$\text{VaR}_\alpha[X] = \sup\{x : \mathbb{P}(X \geq x) \geq \alpha\}, \quad (1)$$

where it is common to have  $\alpha \in [0.9, 1]$ .

Despite the popularity of VaR, optimizing a policy for VaR has several problems: (1) optimizing for VaR results in an NP hard optimization problem (Delage & Mannor, 2010), (2) VaR ignores risk in the tail that occurs with probability

less than  $(1 - \alpha)$  which is problematic for domains where there are rare but potentially catastrophic outcomes, and (3) VaR is not a coherent risk measure (Artzner et al., 1999).

### 3.3.2. CONDITIONAL VALUE AT RISK

CVaR is a coherent risk measure (Delbaen, 2002), also known as average value at risk, expected tail risk, or expected shortfall. For continuous distributions

$$\text{CVaR}_\alpha[X] = \mathbb{E}_{f(X)}[X \mid X \leq \text{VaR}_\alpha[X]]. \quad (2)$$

In addition to being coherent, CVaR can be maximized via convex optimization, does not ignore the tail of the distribution, and is a lower bound on VaR. Because of these desirable properties, we would like to use CVaR as our risk measure. However, because posterior distributions obtained via Bayesian IRL are often discrete (Ramachandran & Amir, 2007; Sadigh et al., 2017; Hadfield-Menell et al., 2017; Brown & Niekum, 2018), we cannot directly optimize for CVaR using the definition in Equation (2) since this definition only works for atomless distributions. Instead, we make use of the following definition of CVaR, proposed by Rockafellar et al. (2000), that works for any distribution:

$$\text{CVaR}_\alpha[X] = \max_{\sigma} \left( \sigma - \frac{1}{1 - \alpha} \mathbb{E}[(\sigma - X)_+] \right), \quad (3)$$

where  $(x)_+ = \max(0, x)$  and  $\sigma$  roughly corresponds to the  $\text{VaR}_\alpha$ . To gain intuition for this formula, note that if we define  $\sigma = \text{VaR}_\alpha[X]$  we can rewrite  $\text{CVaR}_\alpha$  as

$$\begin{aligned} \text{CVaR}_\alpha[X] &= \mathbb{E}_{f(X)}[X \mid X \leq \sigma] \\ &= \sigma - \mathbb{E}_{f(X)}[\sigma - X \mid X \leq \sigma] \\ &= \sigma - \frac{\mathbb{E}_{f(X)}[\mathbf{1}_{X \leq \sigma} \cdot (\sigma - X)]}{P(X \leq \sigma)} \\ &= \sigma - \frac{1}{1 - \alpha} \mathbb{E}_{f(X)}[(\sigma - X)_+] \end{aligned}$$

where  $\mathbf{1}_x = 1$  is the indicator function that evaluates to 1 if  $x$  is True and 0 otherwise, and where we used the linearity of expectation, the definition of conditional expectation, and the definitions of  $\text{VaR}_\alpha[X]$ , and  $(x)_+$ . Taking the maximum over  $\sigma \in \mathbb{R}$ , gives us the definition in Equation (3).

## 4. Bayesian Robust Optimization for Imitation Learning

In Section 4.1 we describe the Bayesian robust optimization for imitation learning (BROIL) objective, previously proposed by (Brown et al., 2020b). Then, in sections 4.2 and 4.3, we derive a novel policy gradient update for BROIL and provide an intuitive explanation for the result.

### 4.1. Soft-Robust BROIL Objective

Rather than seeking a purely risk-sensitive or purely risk-neutral approach, we seek to optimize a soft-robust objective that balances the expected and probabilistic worst-case performance of a policy. Given some performance metric  $\psi(\pi_\theta, R)$  where  $R \sim \mathbb{P}(R)$ , Brown et al. (2020b) recently proposed Bayesian Robust Optimization for Imitation Learning (BROIL) which seeks to optimize the following:

$$\max_{\pi_\theta} \lambda \cdot \mathbb{E}_{\mathbb{P}(R)}[\psi(\pi_\theta, R)] + (1 - \lambda) \cdot \text{CVaR}_\alpha[\psi(\pi_\theta, R)] \quad (4)$$

For MDPs with discrete states and actions and known dynamics, Brown et al. (2020b) showed that this problem can be formulated as a linear program which can be solved in polynomial time. However, many MDPs of interest involve continuous states and actions and unknown dynamics.

### 4.2. BROIL Policy Gradient

We now derive a policy gradient objective for BROIL that allows us to extend BROIL to continuous states and actions and unknown transition dynamics, enabling robust policy learning in a wide variety of practical settings. Given a parameterized policy  $\pi_\theta$  and  $N$  possible reward hypotheses, there are many possible choices for the performance metric  $\psi(\pi_\theta, R)$ . Brown et al. (2020a) considered two common metrics: (1) expected value, i.e.,  $\psi(\pi_\theta, R) = v(\pi, R) = \mathbb{E}_{\tau \sim \pi_\theta}[R(\tau)]$  and (2) baseline regret, i.e.,  $\psi(\pi_\theta, R) = v(\pi_\theta, R) - v(\pi_E, R)$  where  $\pi_E$  denotes an expert policy (usually estimated from demonstrations). In Appendix A we derive a more general form for any performance metric  $\psi(\pi_\theta, R)$  and also give the derivation for the baseline regret performance metric. For simplicity, we let  $\psi(\pi_\theta, R) = v(\pi, R)$  (expected return) hereafter.

To find the policy that maximizes Equation (4) we need the gradient with respect to the policy parameters  $\theta$ . For the first term in Equation (4), we have

$$\nabla_{\theta} \mathbb{E}_{\mathbb{P}(R)}[v(\pi_\theta, R)] \approx \sum_{i=1}^N \mathbb{P}(r_i) \nabla_{\theta} \mathbb{E}_{\tau \sim \pi_\theta}[r_i(\tau)]. \quad (5)$$

Next, we consider the gradient of the CVaR term. CVaR is not differentiable everywhere so we derive a sub-gradient. Given a finite number of samples from the reward function posterior, we can write this sub-gradient as

$$\nabla_{\theta} \max_{\sigma} \left( \sigma - \frac{1}{1 - \alpha} \sum_{i=1}^N \mathbb{P}(r_i) (\sigma - \mathbb{E}_{\tau \sim \pi_\theta}[r_i(\tau)])_+ \right) \quad (6)$$

where  $(x)_+ = \max(0, x)$ . To solve for the sub-gradient of this term, note that given a fixed policy  $\pi_\theta$ , we can solve for  $\sigma$  via a line search: since the objective is piece-wise



linear we only need to check the value at each point  $v(\pi, r_i)$ , for each reward function sample from the posterior since these are the endpoints of each linear segment. If we let  $v_i = v(\pi, r_i)$  then we can quickly iterate over all reward function hypotheses and solve for  $\sigma$  as

$$\sigma^* = \operatorname{argmax}_{\sigma \in \{v_1, \dots, v_N\}} \left( \sigma - \frac{1}{1 - \alpha} \sum_{i=1}^N \mathbb{P}(r_i) [\sigma - v_i]_+ \right). \quad (7)$$

Solving for  $\sigma^*$  requires estimating  $v_i$  by collecting a set  $\mathcal{T}$  of on-policy trajectories  $\tau \sim \pi_\theta$  where  $\tau = (s_0, a_0, s_1, a_1, \dots, s_T, a_T)$ :

$$v_i \approx \frac{1}{|\mathcal{T}|} \sum_{\tau \in \mathcal{T}} \sum_{t=0}^T r_i(s_t, a_t). \quad (8)$$

Solving for  $\sigma^*$  does not require additional data collection beyond what is required for standard policy gradient approaches. We simply evaluate the set of rollouts  $\mathcal{T}$  from  $\pi_\theta$  under each reward function hypothesis,  $r_i$  and then solve the optimization problem above to find  $\sigma^*$ . While this requires more computation than a standard policy gradient approach—we have to evaluate each rollout under  $N$  reward functions—this does not increase the online data collection, which is often the bottleneck in RL algorithms.

Given the solution  $\sigma^*$  found by solving the optimization problem in (7), we perform a step of policy gradient optimization by following the sub-gradient of CVaR with respect to the policy parameters  $\theta$ :

$$\nabla_\theta \text{CVaR}_\alpha = \frac{1}{1 - \alpha} \sum_{i=1}^N \mathbb{P}(r_i) \mathbf{1}_{\sigma^* \geq v(\pi_\theta, r_i)} \nabla_\theta v(\pi_\theta, r_i) \quad (9)$$

where  $\mathbf{1}_x$  is the indicator function that evaluates to 1 if  $x$  is True and 0 otherwise. Given the sub-gradient of the BROIL objective (9), the only thing remaining to compute is the standard policy gradient. Note that in standard RL, we write the policy gradient as (Sutton & Barto, 2018):

$$\nabla_\theta \mathbb{E}_{\tau \sim \pi_\theta} [R(\tau)] = \mathbb{E}_{\tau \sim \pi_\theta} \left[ \sum_{t=0}^T \nabla_\theta \log \pi_\theta(a_t | s_t) \Phi_t(\tau) \right]$$

where  $\Phi_t$  is a measure of the performance of trajectory  $\tau$  starting at time  $t$ . One of the most common forms of  $\Phi_t(\tau)$  is the on-policy advantage function (Schulman et al., 2015) with respect to some single reward function:

$$\Phi_t(\tau) = A^{\pi_\theta}(s_t, a_t) = Q^{\pi_\theta}(s_t, a_t) - V^{\pi_\theta}(s_t). \quad (10)$$

If we define  $\Phi_t^{r_i}$  in terms of a particular reward function  $r_i$ , then, as we show in Appendix A, we can rearrange terms in the standard policy gradient formula to obtain the following form for the BROIL policy gradient which we

estimate using a set  $\mathcal{T}$  of on-policy trajectories  $\tau \sim \pi_\theta$  where  $\tau = (s_0, a_0, s_1, a_1, \dots, s_T, a_T)$  as follows:

$$\nabla_\theta \text{BROIL} \approx \frac{1}{|\mathcal{T}|} \sum_{\tau \in \mathcal{T}} \left[ \sum_{t=0}^T \nabla_\theta \log \pi_\theta(a_t | s_t) w_t(\tau) \right] \quad (11)$$

where

$$w_t(\tau) = \sum_{i=1}^N \mathbb{P}(r_i) \Phi_t^{r_i}(\tau) \left( \lambda + \frac{1 - \lambda}{1 - \alpha} \mathbf{1}_{\sigma^* \geq v(\pi, r_i)} \right) \quad (12)$$

is the weight associated with each state-action pair  $(s_t, a_t)$  in the set of trajectory rollouts  $\mathcal{T}$ . The resulting vanilla policy gradient algorithm is summarized in Algorithm 1. In Appendix C we show how to apply a trust-region update based on Proximal Policy Optimization (Schulman et al., 2017b) for more stable policy gradient optimization.

### 4.3. Intuitive Interpretation of the Policy Gradient

Consider the policy gradient weight  $w_t$  given in Equation (12). If  $\lambda = 1$ , then

$$w_t(\tau) = \sum_{i=1}^N \mathbb{P}(R_i) \Phi_t^{R_i}(\tau) = \Phi_t^{\bar{R}}(\tau) \quad (13)$$

where  $\bar{R}$  is the expected reward under the posterior. Thus,  $\lambda = 1$  is equivalent to standard policy gradient optimization under the mean reward function and gradient ascent will focus on increasing the likelihood of actions that look good in expectation over the reward function distribution  $\mathbb{P}(R)$ . Alternatively, if  $\lambda = 0$ , then

$$w_t(\tau) = \frac{1}{1 - \alpha} \sum_{i=1}^N \mathbf{1}_{\sigma^* \geq v(\pi, R_i)} \mathbb{P}(R_i) \Phi_t^{R_i}(\tau) \quad (14)$$

and gradient ascent will increase the likelihood of actions that look good under reward functions that the current policy  $\pi_\theta$  performs poorly under, i.e., policy gradient updates will focus on improving performance under all  $R_i$  such that  $v(\pi, R_i) \leq \sigma^*$ , weighting the gradient according to the likelihood of these worst-case reward functions. The update rule also multiplies by  $1/(1 - \alpha)$  which acts to normalize the magnitude of the gradient: as  $\alpha \rightarrow 1$  we update on reward functions further into the tail, which have smaller probability mass. Thus,  $\lambda \in [0, 1]$  allows us to blend between maximizing policy performance in expectation versus worst-case and  $\alpha \in [0, 1)$  determines how far into the tail of the distribution to focus the worst-case updates.

## 5. Experiments

In experiments, we consider the following questions: (1) Can PG-BROIL learn control policies in MDPs with continuous states and actions and unknown transition dynamics?

**Algorithm 1** Policy Gradient BROIL

- 1: **Input:** initial policy parameters  $\theta_0$ , samples from reward function posterior  $r_1, \dots, r_N$  and associated probabilities,  $\mathbb{P}(r_1), \dots, \mathbb{P}(r_N)$ .
- 2: **for**  $k = 0, 1, 2, \dots$  **do**
- 3:   Collect set of trajectories  $\mathcal{T}_k = \{\tau_i\}$  by running policy  $\pi_{\theta_k}$  in the environment.
- 4:   Estimate expected return of  $\pi_{\theta_k}$  under each reward function hypothesis  $r_j$  using Eq. (8).
- 5:   Solve for  $\sigma^*$  using Eq. (7)
- 6:   Estimate policy gradient using Eq. (11) and Eq. (12).
- 7:   Update  $\theta$  using gradient ascent.
- 8: **end for**

(2) Does optimizing PG-BROIL with different values of  $\lambda$  effectively trade-off between maximizing for expected return and maximizing robustness? (3) When demonstrations are ambiguous, can PG-BROIL outperform other imitation learning baselines by hedging against uncertainty? Code and videos are available at <https://sites.google.com/view/pg-broil>.

**5.1. Prior over Reward Functions**

We first consider an RL agent with a priori uncertainty over the true reward function. This setting allows us to initially avoid the difficulties of inferring a posterior distribution over reward functions and carefully examine whether PG-BROIL can trade-off expected performance and robustness (CVaR) under epistemic uncertainty over the true reward function. We study 3 domains: the classical CartPole benchmark (Brockman et al., 2016), a pointmass navigation task inspired by (Thananjeyan et al., 2020b) and a robotic reaching task from the DM Control Suite (Tassa et al., 2020). All domains are characterized by a robot navigating in an environment where some states have uncertain costs. All domains have unknown transition dynamics and continuous states and actions (except CartPole which has discrete actions). We implement PG-BROIL on top of OpenAI Spinning Up (Achiam, 2018). For cartpole we implement PG-BROIL on top of REINFORCE (Peters & Schaal, 2008) and for remaining domains we implement PG-BROIL on top of PPO (Schulman et al., 2017b) (see Appendix C).

5.1.1. EXPERIMENTAL DOMAINS

**CartPole:** We consider a risk-sensitive version of the classic CartPole benchmark (Brockman et al., 2016). The reward function is  $R(s) = b \cdot s_x$ , where  $s_x$  is the position of the cart on the track, and there is uncertainty over  $b$ . Our prior over  $b$  is distributed uniformly in the range  $[-1, 0.2]$ . The center of the track is  $s_x = 0$ . We sample values of  $b$  between -1 and 0.2 across even intervals of 0.2 width to form a discrete posterior distribution for PG-BROIL. The reward distribution

is visualized in Figure 2a. Based on our prior distribution over reward functions, the left side of the track ( $s_x < 0$ ) is associated with a higher expected reward but a worse worst case scenario (the potential for negative rewards). By contrast, the robust solution is to stay in the middle of the track in order to perform well across all possible reward functions since the center of the track has less risk of a significantly negative reward than the left or right sides of the track.

**Pointmass Navigation:** We next consider a risk-sensitive continuous 2-D navigation task inspired by Thananjeyan et al. (2020b). Here the objective is to control a pointmass robot towards a known goal location with forces in cardinal directions in a system with linear Gaussian dynamics and drag. There are gray regions of uncertain cost that can either be traversed or avoided as illustrated in Figure 2b. For example, these regions could represent grassy areas which are likely easy to navigate, but where the grass may occlude mud or holes which would impede progress and potentially cause damage or undue wear and tear on the robot. The robot has prior knowledge that it needs to reach the goal location  $g = (0, 0)$  on the map, depicted by the red star. We represent this prior with a nominal cost for each step that is the distance to the goal from the robot’s position. We add a penalty term of uncertain cost for going through the gray region giving the following reward function posterior:

$$R(s) = - (\|s_{x,y} - g\|_2^2 + b \cdot \mathbf{1}_{\text{gray}}), b \sim \mathbb{P}(b), \quad (15)$$

where  $\mathbf{1}_{\text{gray}}$  is an indicator for entering a gray region, and where the distribution  $\mathbb{P}(b)$  over the penalty  $b$  is given as

$b$	-500	-40	0	40	50
$\mathbb{P}(b)$	0.05	0.05	0.2	0.3	0.4

On average it is favorable to go through the gray region ( $\mathbb{E}[b] = +5$ ), but there is some probability that going through the gray region is highly unfavorable:

**Reacher:** We design a modified version of the Reacher environment from the DeepMind Control Suite (Tassa et al., 2020) (Figure 2c), which is a 2 link planar arm where the robot can apply joint torques to each of the 2 joints to guide the end effector of the arm to a goal position on the plane. We modify the original environment by including an area of uncertainty (large red circle). When outside the uncertain region, the robot receives a reward which penalizes the distance between the end effector and the goal (small yellow circle). Thus, the robot is normally incentivized to guide the end effector to the goal as quickly as possible. When the end effector is inside the uncertain region, the robot has an 80% chance of receiving a +2 bonus, a 10% chance of receiving a -2 penalty, and a 10% chance of neither happening (receiving rewards as if it were outside the uncertain region). The large red circle can be interpreted as a region on the table that has a small chance of causing harm to the robot or breaking

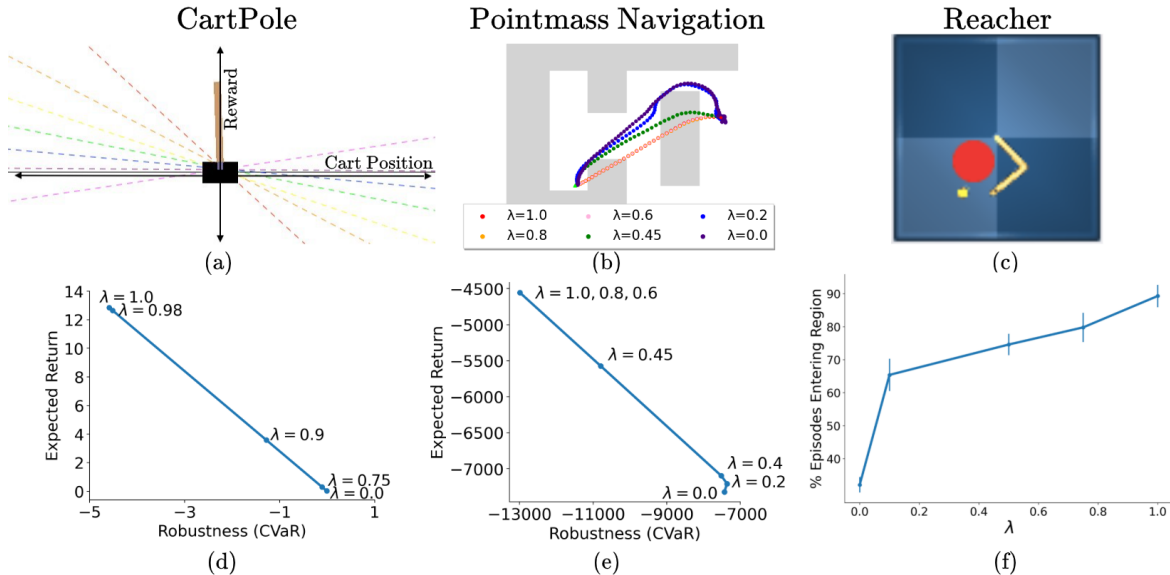


**Figure 2. Prior over Reward Functions: Domains and Results.** We study (a) CartPole in which the reward is an unknown linear function of the cart’s position, (b) Pointmass Navigation with gray regions of uncertain costs, and (c) Reacher with a red region of uncertain cost. For the CartPole and Pointmass Navigation domains, we find that as  $\lambda$  is decreased, the learned policy optimizes more for being robust to tail risk and thus achieves more robust performance (in terms of CVaR) at the expense of expected return in panels (d) and (e). In panel (f), we find that the reacher arm enters the riskier red region less often with decreasing  $\lambda$  as expected.

an object on the table. However, in expectation the robot believes it is good to enter the red region (e.g., assuming that objects in this region are not fragile).

### 5.1.2. RESULTS

PG-BROIL consistently exhibits more risk-averse behaviors with decreasing  $\lambda$  across all domains. For CartPole and Pointmass Navigation, we see that as  $\lambda$  is decreased, the learned policy becomes more robust to tail risk at the expense of lower expected return in Figures 2d and 2e respectively. Figure 2e indicates that values of  $\lambda$  close to 0 can lead to unstable policy optimization due to excessive focus on tail risk—the policy for  $\lambda = 0$  is Pareto dominated by the policy for  $\lambda = 0.2$ . We visualize the learned behaviors for different values of  $\lambda$  for the Pointmass Navigation environment in Figure 2b. For high values of  $\lambda$ , the robot cuts straight through the uncertain terrain, for intermediate values (eg.  $\lambda = 0.45$ ), the robot somewhat avoids the uncertain terrain, while for low values of  $\lambda$ , the robot almost entirely avoids the uncertain terrain at the expense of a longer path. Finally, for the Reacher environment, we find that the percentage of episodes where the arm enters the red region decreases as  $\lambda$  decreases as expected (Figure 2f).

## 5.2. Learning from Demonstrations

Our previous results demonstrated that PG-BROIL is able to learn policies that effectively balance expected performance and robustness in continuous MDPs under a given

prior over reward functions. In this section, we consider the imitation learning setting where a robot infers a reward function from demonstrated examples. Given such input, there are typically many reward functions that are consistent with it; however, many reward inference algorithms (Fu et al., 2017; Finn et al., 2016; Brown et al., 2019) will output only one of them—not necessarily the true reward. There has been some work on Bayesian algorithms such as Bayesian IRL (Ramachandran & Amir, 2007) which estimates a *posterior distribution* instead of a single reward and Bayesian REX (Brown et al., 2020a) which makes it possible to efficiently learn this posterior from preferences over high dimensional demonstrated examples of varying qualities. However, prior work on Bayesian reward learning often only optimizes policies for the expected or MAP reward estimate over the learned posterior (Ramachandran & Amir, 2007; Choi & Kim, 2011; Brown et al., 2020a). Our hypothesis is that for imitation learning problems with high uncertainty about the true reward function, taking a robust optimization approach via PG-BROIL will lead to better performance by producing policies that do well in expectation, but also avoid low reward under *any* of the sufficiently probable reward functions in the learned posterior.

### 5.2.1. TRASHBOT FROM DEMOS

We first consider a continuous control TrashBot domain (Figure 3), where aim to teach a robot to pick up pieces of trash (black dots) while avoiding the gray boundary regions. The state-space, dynamics and actions are the same as for

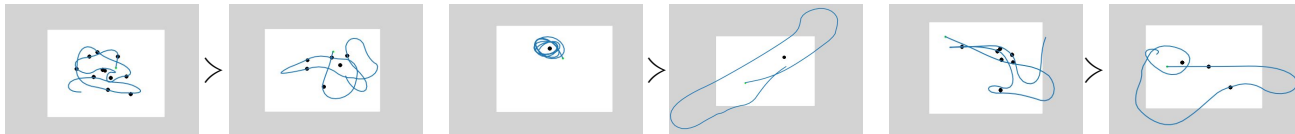


Figure 3. **TrashBot environment:** Each time the robot picks up a piece of trash (by moving close to a black dot), a new one appears at a randomly in the white region. We give pairwise preferences over human demos that aim to teach the robot that picking up trash is good (left), going into the gray region is undesirable (center), and less time in the gray region and picking up more trash is preferred (right).

Table 1. **TrashBot:** We evaluate PG-BROIL against 5 other imitation learning algorithms when learning from ambiguous preferences over demonstrations (Figure 3). Results are averages ( $\pm$  one st. dev.) over 10 random seeds and 100 test episodes each with a horizon of 100 steps per episode. For PG-BROIL, we set  $\alpha = 0.95$  and report results for the best  $\lambda$  ( $\lambda = 0.8$ ).

ALGORITHM	AVG. TRASH COLLECTED	AVG. STEPS IN GRAY REGION
BC	$3.4 \pm 1.8$	$2.7 \pm 6.2$
GAIL	$2.2 \pm 1.5$	$3.7 \pm 9.9$
RAIL	$1.1 \pm 1.2$	$2.2 \pm 6.9$
PBRL	$2.6 \pm 1.5$	$1.2 \pm 2.7$
BAYESIAN REX	$1.6 \pm 1.3$	$1.2 \pm 1.7$
<b>PG-BROIL</b>	<b><math>8.4 \pm 0.5</math></b>	<b><math>0.1 \pm 0.1</math></b>

the Pointmass Navigation environment and we provide human demonstrations via a simple teleoperation interface. The robot constructs its reward function hypotheses as linear combinations of three binary features which correspond to: (1) being in the gray region (GRAY), (2) being in the white region (WHITE), and (3) picking up a piece of trash (TRASH). We give three pairwise preferences over human teleoperated trajectories (generated by one of the authors) as shown in Figure 3. However, the small number of preferences makes it challenging for the robot to ascertain the true reward function parameters as there are many reward function weights that would lead to the same human preferences. Furthermore, the most salient feature is WHITE and this feature is highly correlated, but not causal, with the preferences. Thus, this domain can easily lead to reward hacking/gaming behaviors (Krakovna et al., 2020). We hypothesize that PG-BROIL will hedge against uncertainty and learn to pick up trash while avoiding the gray region.

We compare against behavioral cloning (BC), GAIL (Ho & Ermon, 2016), and Risk-Averse Imitation Learning (RAIL) (Santara et al., 2018), which estimates CVaR over trajectories to create a risk-averse version of the GAIL algorithm. To facilitate a fairer comparison, we only give BC, GAIL, and RAIL the better ranked demonstration from each preference pair. We also compare with Preference-based RL (PBRL) (Christiano et al., 2017) in the offline demonstration setting (Brown et al., 2019) which optimizes an MLE estimate of the reward weights and Bayesian REX (Brown

et al., 2020a), which optimizes the mean reward function under the posterior distribution given the preferences. PG-BROIL also uses Bayesian REX (Brown et al., 2020a) to infer a reward function posterior distribution given the preferences over demonstrations (see Appendix E for details), but optimizes the BROIL objective.

Table 1 compares the performance of each baseline imitation learning algorithm when given the 3 pairs of demonstrations shown in Figure 3. We find that PG-BROIL outperforms BC and GAIL (Ho & Ermon, 2016) by not directly seeking to imitate the states and actions in the demonstrations, but by explicitly reasoning about uncertainty in the true reward function. We also find that PG-BROIL significantly outperforms RAIL. This is because RAIL only focuses on minimizing aleatoric uncertainty under stochastic transition dynamics for a single reward function (the discriminator), not epistemic uncertainty over the true reward function. We find that PG-BROIL outperforms PBRL and Bayesian REX.

We inspected the learned reward functions and found that the PBRL reward places heavy emphasis on collecting trash but has a small positive weight on the WHITE feature. We hypothesize that this results in policy optimization falling into a local maxima in which it mostly mines rewards by staying in the white region. By contrast, PG-BROIL considers a number of reward hypotheses, many of which have negative weights on the WHITE feature. Thus, a risk-averse agent cannot mine rewards by simply staying in the white region, and is incentivized to maximally pick up trash while keeping visits to the gray region low. The mean reward function optimized by Bayesian REX penalizes visiting the gray region but learns roughly equal weights for the WHITE and TRASH features. Thus, Bayesian REX is not strongly incentivized to pick up trash. Because of this the learned policy sometimes visits the borders of the white region and occasionally enters the gray region when it accumulates too high of a velocity. By contrast, PG-BROIL effectively optimizes a policy that is robust to multiple hypotheses that explain the rankings: picking up trash more than any other policy, while avoiding the gray region. See Appendix F.

### 5.2.2. REACHER FROM DEMOS WITH DOMAIN SHIFT

For this experiment, we use the same Reacher environment described above. We give the agent five pairwise prefer-



Table 2. **Reacher from Demos:** We evaluate PG-BROIL and baseline imitation learning algorithms when learning from preferences over demonstrations. Results are averages ( $\pm$  one st. dev.) over 3 seeds and 100 test episodes with a horizon of 200 steps per episode. For PG-BROIL, we set  $\alpha = 0.9$  and report results for  $\lambda = 0.15$ .

ALGORITHM	AVG. STEPS IN UNCERTAIN REGION	AVG. STEPS IN TARGET REGION
BC	11.3 $\pm$ 27.4	39.9 $\pm$ 62.3
GAIL	2.3 $\pm$ 1.7	5.1 $\pm$ 13.0
RAIL	2.1 $\pm$ 1.2	4.6 $\pm$ 27.0
PBRL	28.4 $\pm$ 37.7	16.8 $\pm$ 30.4
BAYESIAN REX	13.5 $\pm$ 35.0	94.5 $\pm$ 70.1
<b>PG-BROIL</b>	<b>1.7 <math>\pm</math> 7.2</b>	<b>102.0 <math>\pm</math> 60.5</b>

ences over demonstrations of varying quality in a training domain where the uncertain reward region is never close to the goal and where none of the demonstrations show the reacher arm entering the uncertain region. We then introduce domain shift by both optimizing and testing policies in reacher environments unseen in the demonstrations, where the goal location is randomized and sometimes the uncertain reward region is in between the the reacher arm and the goal. The inferred reward function is a linear combination of 2 features: TARGET and UNCERTAIN REGION which are simply binary indicators which identify whether the agent is in the target location or in the uncertain region respectively. In the posterior generated using Bayesian REX, we find that the weight learned for the TARGET feature is strongly positive over all reward functions. UNCERTAIN REGION, having no information from any of the demonstrations, has a wide variety of possible values from -1 to +1 (reward weights are normalized to have unit L2-norm). Both the mean and MLE reward functions assign a positive weight to both the TARGET and UNCERTAIN REGION features, resulting in Bayesian REX and PBRL frequently entering the uncertain region as shown in Table 2. By contrast, PG-BROIL hedges against its uncertainty over the quality of the uncertain region and avoids it. See Appendix D.3.

### 5.2.3. ATARI BOXING FROM DEMOS

For this experiment, we give the agent 3 preferences over suboptimal demos of the Atari Boxing game (Bellemare et al., 2013). We use Bayesian REX to infer a reward function posterior where each inferred reward functions is a linear combinations of 3 binary indicator features identifying whether the agent hit its opponent, got hit, or stayed away from the opponent. The mean and MLE reward functions both assign a high weight to hitting the opponent, ignoring the risk of getting hit by the opponent due to always staying close to the opponent in order to score hits on it. PG-BROIL tries to satisfy multiple reward functions by both trying to avoid getting hit and scoring hits, resulting in better per-



(a)

ALGORITHM	GAME SCORE
BC	1.7 $\pm$ 5.3
GAIL	-0.2 $\pm$ 5.8
RAIL	0.5 $\pm$ 4.9
PBRL	-15.0 $\pm$ 8.2
BAYESIAN REX	1.6 $\pm$ 4.7
<b>PG-BROIL</b>	<b>23.9 <math>\pm</math> 13.5</b>

(b)

Figure 4. **Atari Boxing:** We evaluate PG-BROIL against baseline imitation learning algorithms when learning from preferences over demonstrations. Results are averages ( $\pm$  one st. dev.) over 3 random seeds and 100 test episodes. For PG-BROIL, we set  $\alpha = 0.9$  and report results for the best  $\lambda$  ( $\lambda = 0.3$ ). The game score is the number of hits the trained agent (white) scored minus the number of times the agent gets hit by the opponent (black).

formance under the true reward as shown in Table 4. See Appendix D.5 for more details.

## 6. Discussion and Future Work

**Summary:** We derive a novel algorithm, PG-BROIL, for safe policy optimization in continuous MDPs that is robust to epistemic uncertainty over the true reward function. Experiments evaluating PG-BROIL with different prior distributions over reward hypotheses suggest that solving PG-BROIL with different values of  $\lambda$  can produce a family of solutions that span the Pareto frontier of policies which trade-off expected performance and robustness. Finally, we show that PG-BROIL improves upon state-of-the-art imitation learning methods when learning from small numbers of demonstrations by not just optimizing for the most likely reward function, but by also hedging against poor performance under other likely reward functions.

**Future Work and Limitations:** We found that PG-BROIL can sometimes become unstable for values of lambda close to zero—likely due to the indicator function in the CVaR policy gradient. We experimented with entropic risk measure (Föllmer & Knispel, 2011), a continuously differentiable alternative to CVaR, but obtained similar results to CVaR (see Appendix B). Future work also includes using contrastive learning (Laskin et al., 2020) and deep Bayesian reward function inference (Brown et al., 2020a) to enable robust policy learning from raw pixels.

## Acknowledgements

This work was supported in part by NSF SCHool, AFOSR, ONR YIP, NSF Grants IIS-1717368 and IIS-1815275 and donations from Google, Siemens, Amazon Robotics, Toyota Research Institute, and by equipment grants from NVidia.

## References

- Abbeel, P. and Ng, A. Y. Apprenticeship learning via inverse reinforcement learning. In *Proceedings of the twenty-first international conference on Machine learning*, pp. 1, 2004.
- Achiam, J. Spinning Up in Deep Reinforcement Learning. 2018. URL <https://spinningup.openai.com/>.
- Achiam, J., Held, D., Tamar, A., and Abbeel, P. Constrained policy optimization. In *International Conference on Machine Learning*, pp. 22–31. PMLR, 2017.
- Amodei, D., Olah, C., Steinhardt, J., Christiano, P., Schulman, J., and Mané, D. Concrete problems in ai safety. *arXiv preprint arXiv:1606.06565*, 2016.
- Arora, S. and Doshi, P. A survey of inverse reinforcement learning: Challenges, methods and progress. *arXiv preprint arXiv:1806.06877*, 2018.
- Artzner, P., Delbaen, F., Eber, J.-M., and Heath, D. Coherent measures of risk. *Mathematical finance*, 9(3):203–228, 1999.
- Bellemare, M. G., Naddaf, Y., Veness, J., and Bowling, M. The arcade learning environment: An evaluation platform for general agents. *Journal of Artificial Intelligence Research*, 47:253–279, 2013.
- Brockman, G., Cheung, V., Pettersson, L., Schneider, J., Schulman, J., Tang, J., and Zaremba, W. Openai gym, 2016.
- Brown, D., Goo, W., Nagarajan, P., and Niekum, S. Extrapolating beyond suboptimal demonstrations via inverse reinforcement learning from observations. In *International Conference on Machine Learning*, pp. 783–792. PMLR, 2019.
- Brown, D., Niekum, S., Coleman, R., and Srinivasan, R. Safe imitation learning via fast bayesian reward inference from preferences. In *International Conference on Machine Learning*, 2020a.
- Brown, D., Niekum, S., and Marek, P. Bayesian robust optimization for imitation learning. In *Neural Information Processing Systems (NeurIPS)*, 2020b.
- Brown, D. S. and Niekum, S. Efficient probabilistic performance bounds for inverse reinforcement learning. In *Thirty-Second AAAI Conference on Artificial Intelligence*, 2018.
- Choi, J. and Kim, K.-E. Map inference for bayesian inverse reinforcement learning. In *Advances in Neural Information Processing Systems*, pp. 1989–1997, 2011.
- Christiano, P., Leike, J., Brown, T. B., Martic, M., Legg, S., and Amodei, D. Deep reinforcement learning from human preferences. *arXiv preprint arXiv:1706.03741*, 2017.
- Delage, E. and Mannor, S. Percentile optimization for markov decision processes with parameter uncertainty. *Operations research*, 58(1):203–213, 2010.
- Delbaen, F. Coherent risk measures on general probability spaces. In *Advances in finance and stochastics*, pp. 1–37. Springer, 2002.
- Derman, E., Mankowitz, D. J., Mann, T. A., and Mannor, S. Soft-robust actor-critic policy-gradient. *arXiv preprint arXiv:1803.04848*, 2018.
- Finn, C., Levine, S., and Abbeel, P. Guided cost learning: Deep inverse optimal control via policy optimization. In *International conference on machine learning*, pp. 49–58. PMLR, 2016.
- Fisac, J. F., Akametalu, A. K., Zeilinger, M. N., Kaynama, S., Gillula, J., and Tomlin, C. J. A general safety framework for learning-based control in uncertain robotic systems. In *IEEE Transactions on Automatic Control*, 2018.
- Föllmer, H. and Knispel, T. Entropic risk measures: Coherence vs. convexity, model ambiguity and robust large deviations. *Stochastics and Dynamics*, 11(02n03):333–351, 2011.
- Fu, J., Luo, K., and Levine, S. Learning robust rewards with adversarial inverse reinforcement learning. *arXiv preprint arXiv:1710.11248*, 2017.
- Garcia, J. and Fernández, F. A comprehensive survey on safe reinforcement learning. *Journal of Machine Learning Research*, 16(1):1437–1480, 2015.
- Griffith, S., Subramanian, K., Scholz, J., Isbell, C. L., and Thomaz, A. Policy shaping: integrating human feedback with reinforcement learning. In *Proceedings of the 26th International Conference on Neural Information Processing Systems-Volume 2*, pp. 2625–2633, 2013.
- Haarnoja, T., Zhou, A., Abbeel, P., and Levine, S. Soft actor-critic: Off-policy maximum entropy deep reinforcement learning with a stochastic actor, 2018.
- Hadfield-Menell, D., Milli, S., Abbeel, P., Russell, S. J., and Dragan, A. Inverse reward design. In *Advances in neural information processing systems*, pp. 6765–6774, 2017.
- Heger, M. Consideration of risk in reinforcement learning. In *Machine Learning Proceedings*, 1994.

- Ho, J. and Ermon, S. Generative Adversarial Imitation Learning. In *Advances in Neural Information Processing Systems*, pp. 7461–7472, 2016.
- Hoque, R., Balakrishna, A., Putterman, C., Luo, M., Brown, D. S., Seita, D., Thananjeyan, B., Novoseller, E., and Goldberg, K. Lazydagger: Reducing context switching in interactive imitation learning. *arXiv preprint arXiv:2104.00053*, 2021.
- Huang, J., Wu, F., Precup, D., and Cai, Y. Learning safe policies with expert guidance. In *Advances in Neural Information Processing Systems*, pp. 9105–9114, 2018.
- Hussein, A., Gaber, M. M., Elyan, E., and Jayne, C. Imitation learning: A survey of learning methods. *ACM Computing Surveys (CSUR)*, 50(2):1–35, 2017.
- Knox, W. B. and Stone, P. Reinforcement learning from simultaneous human and mdp reward. In *AAMAS*, pp. 475–482, 2012.
- Krakovna, V., Uesato, J., Mikulik, V., Rahtz, M., Everitt, T., Kumar, R., Kenton, Z., Leike, J., and Legg, S. Specification gaming examples in ai. DeepMind Blog, 2020.
- Lacotte, J., Ghavamzadeh, M., Chow, Y., and Pavone, M. Risk-sensitive generative adversarial imitation learning. *arXiv preprint arXiv:1808.04468*, 2018.
- Laskin, M., Srinivas, A., and Abbeel, P. Curl: Contrastive unsupervised representations for reinforcement learning. In *International Conference on Machine Learning*, pp. 5639–5650. PMLR, 2020.
- Lobo, E. A., Ghavamzadeh, M., and Petrik, M. Soft-robust algorithms for handling model misspecification. *arXiv preprint arXiv:2011.14495*, 2020.
- Majumdar, A., Singh, S., Mandlekar, A., and Pavone, M. Risk-sensitive inverse reinforcement learning via coherent risk models. In *Robotics: Science and Systems*, 2017.
- Nass, D., Belousov, B., and Peters, J. Entropic risk measure in policy search. *arXiv preprint arXiv:1906.09090*, 2019.
- Osa, T., Pajarinen, J., Neumann, G., Bagnell, J. A., Abbeel, P., and Peters, J. An algorithmic perspective on imitation learning. *arXiv preprint arXiv:1811.06711*, 2018.
- Peters, J. and Schaal, S. Reinforcement Learning of Motor Skills with Policy Gradients. *Neural Networks*, 21(4): 682–697, 2008.
- Pomerleau, D. A. Efficient training of artificial neural networks for autonomous navigation. *Neural computation*, 3(1):88–97, 1991.
- Puterman, M. L. *Markov decision processes: Discrete stochastic dynamic programming*. Wiley-Interscience, 2005.
- Ramachandran, D. and Amir, E. Bayesian inverse reinforcement learning. In *IJCAI*, volume 7, pp. 2586–2591, 2007.
- Ratner, E., Hadfield-Mennell, D., and Dragan, A. Simplifying reward design through divide-and-conquer. In *Robotics: Science and Systems*, 2018.
- Regan, K. and Boutilier, C. Regret-based reward elicitation for Markov decision processes. In *Conference on Uncertainty in Artificial Intelligence (UAI)*, pp. 444–451, 2009. ISBN 978-0-9749039-5-8.
- Rockafellar, R. T., Uryasev, S., et al. Optimization of conditional value-at-risk. *Journal of risk*, 2:21–42, 2000.
- Ross, S. and Bagnell, D. Efficient reductions for imitation learning. In *Proceedings of the thirteenth international conference on artificial intelligence and statistics*, pp. 661–668. JMLR Workshop and Conference Proceedings, 2010.
- Ross, S., Gordon, G., and Bagnell, D. A reduction of imitation learning and structured prediction to no-regret online learning. In *Proceedings of the fourteenth international conference on artificial intelligence and statistics*, pp. 627–635. JMLR Workshop and Conference Proceedings, 2011.
- Russel, R. H., Behzadian, B., and Petrik, M. Entropic risk constrained soft-robust policy optimization. *arXiv preprint arXiv:2006.11679*, 2020.
- Sadigh, D., Dragan, A. D., Sastry, S., and Seshia, S. A. Active preference-based learning of reward functions. In *Robotics: Science and Systems*, 2017.
- Santara, A., Naik, A., Ravindran, B., Das, D., Mudigere, D., Avancha, S., and Kaul, B. RAIL : Risk-Averse Imitation Learning Extended Abstract. *arXiv:1707.06658*, 2018.
- Schulman, J., Moritz, P., Levine, S., Jordan, M., and Abbeel, P. High-dimensional continuous control using generalized advantage estimation. *arXiv preprint arXiv:1506.02438*, 2015.
- Schulman, J., Levine, S., Moritz, P., Jordan, M. I., and Abbeel, P. Trust region policy optimization. *arXiv preprint arXiv:1707.06347*, 2017a.
- Schulman, J., Wolski, F., Dhariwal, P., Radford, A., and Klimov, O. Proximal policy optimization algorithms. *arXiv preprint arXiv:1707.06347*, 2017b.

- Shen, Y., Tobia, M. J., Sommer, T., and Obermayer, K. Risk-sensitive reinforcement learning. In *Neural Computation*, volume 26, 2014.
- Sutton, R. S. and Barto, A. G. *Reinforcement learning: An introduction*. MIT press, 2018.
- Syed, U., Bowling, M., and Schapire, R. E. Apprenticeship learning using linear programming. In *Proceedings of the 25th international conference on Machine learning*, pp. 1032–1039, 2008.
- Tamar, A., Glassner, Y., and Mannor, S. Policy gradients beyond expectations: Conditional value-at-risk. In *CoRR*, 2014.
- Tamar, A., Glassner, Y., and Mannor, S. Optimizing the cvar via sampling. In *Twenty-Ninth AAAI Conference on Artificial Intelligence*, 2015.
- Tang, Y. C., Zhang, J., and Salakhutdinov, R. Worst cases policy gradients. *Conf. on Robot Learning (CoRL)*, 2019.
- Tang, Y. C., Zhang, J., and Salakhutdinov, R. Worst cases policy gradients. In Kaelbling, L. P., Kragic, D., and Sugiura, K. (eds.), *Proceedings of the Conference on Robot Learning*, volume 100 of *Proceedings of Machine Learning Research*, pp. 1078–1093. PMLR, 30 Oct–01 Nov 2020. URL <http://proceedings.mlr.press/v100/tang20a.html>.
- Tassa, Y., Tunyasuvunakool, S., Muldal, A., Doron, Y., Liu, S., Bohez, S., Merel, J., Erez, T., Lillicrap, T., and Heess, N. *dm\_control: Software and tasks for continuous control*, 2020.
- Thananjeyan, B., Balakrishna, A., Rosolia, U., Gonzalez, J. E., Ames, A., and Goldberg, K. Abc-mpc: Safe sample-based learning mpc for stochastic nonlinear dynamical systems with adjustable boundary conditions. In *Workshop on the Algorithmic Foundations of Robotics*, 2020a.
- Thananjeyan, B., Balakrishna, A., Rosolia, U., Li, F., McAllister, R., Gonzalez, J. E., Levine, S., Borrelli, F., and Goldberg, K. Safety augmented value estimation from demonstrations (saved): Safe deep model-based rl for sparse cost robotic tasks. *Robotics and Automation Letters (RAL)*, 2020b.
- Thananjeyan, B., Balakrishna, A., Nair, S., Luo, M., Srinivasan, K., Hwang, M., Gonzalez, J. E., Ibarz, J., Finn, C., and Goldberg, K. Recovery rl: Safe reinforcement learning with learned recovery zones. In *Robotics and Automation Letters (RA-L)*. IEEE, 2021.
- Torabi, F., Warnell, G., and Stone, P. Behavioral cloning from observation. In *Proceedings of the 27th International Joint Conference on Artificial Intelligence*, pp. 4950–4957, 2018.
- Xu, K., Ratner, E., Dragan, A., Levine, S., and Finn, C. Learning a prior over intent via meta-inverse reinforcement learning. *International Conference on Machine Learning*, 2019.
- Yuan, Y. Pytorch implementation of reinforcement learning algorithms. <https://github.com/Khrylx/PyTorch-RL>, 2019.
- Zhang, J. and Cho, K. Query-efficient imitation learning for end-to-end autonomous driving. *arXiv preprint arXiv:1605.06450*, 2016.
- Zhang, S., Liu, B., and Whiteson, S. Mean-variance policy iteration for risk-averse reinforcement learning. In *Conference on Artificial Intelligence (AAAI)*, 2021.
- Ziebart, B. D., Maas, A. L., Bagnell, J. A., and Dey, A. K. Maximum entropy inverse reinforcement learning. In *Aaai*, volume 8, pp. 1433–1438. Chicago, IL, USA, 2008.